RSC Advances

ROYAL SOCIETY
OF CHEMISTRY

REVIEW

View Article Online
View Journal | View Issue

Check for updates

Cite this: *RSC Adv.*, 2025, **15**, 42331

Recent progress in carbon coating and surface modification of $LiFePO_4$ cathodes

Sania Ishtiaq,[a] Abdul Majid, *[a] Abdul Qadeer,[b] Mohammad Alkhedher [c]
and Niyazi Bulut[d]

Received 9th August 2025
Accepted 24th October 2025

DOI: 10.1039/d5ra05833c

rsc.li/rsc-advances

Lithium iron phosphate ($LiFePO_4$, LFP) is widely recognized as a cathode material for lithium-ion batteries (LIBs) owing to its excellent high temperature stability, environmental compatibility and impressive cycle retention. Nevertheless, the limited lithium-ion migration rate and poor electronic/ionic conductivities of this material restrict its practical application. This review explores different methods for synthesizing LFP, such as hydrothermal, sol–gel, microwave-assisted, and carbon reduction techniques, assessing them in terms of structural control, scalability, and performance. Additionally, it highlights modification strategies that have evolved from traditional carbon coating to more advanced techniques, such as heteroatom doping in carbon layers, the integration of multi-walled carbon nanotubes (MWCNTs), and thin oxide nanoscale coatings. In this review, the advancements in utilization of LFP for conventional LIB applications as well as in all solid state lithium batteries (ASSLBs) are highlighted, pointing toward future directions for high performance and durable energy storage technologies.

1. Introduction

Lithium-ion batteries (LIBs) are the industry standard for innovative gadgets, handheld appliances, and hybrid or all-electric automobiles owing to their remarkable specific energy and power density properties.[1–3] As shown in Fig. 1, lithium ions move through the electrolyte from the cathode to the anode during charging and reverse direction during discharging. The four main components of a standard LIB are an electrolyte, an anode, a separator, and a cathode. The separator, a porous insulating layer, allows the transport of Li-ions while preventing direct electrode contact and short circuits.[4]

Cathode properties largely determine LIBs performance.[5] Currently, widely used cathode active components in LIBs are generally divided into three major kinds based on their crystal frameworks (1) olivine framework (*e.g.*, $LiFePO_4$), (2) spinel framework (*e.g.*, $LiMn_2O_4$), (3) layered oxide framework (*e.g.*, $LiCoO_2$, $LiNiO_2$, NCA ($LiNiCoAlO_2$), and NCM ($LiNiMnCoO_2$)).[6] Li-ion diffusion channels are two-dimensional in layered oxides but three-dimensional in spinel-type oxides, as discovered in 1983 ref. 7. LFP and other olivine-type oxides were discovered in 1997 and have unidirectional lithium ion flow.[8] Fig. 2 display the crystal frameworks of the three main kinds of Li insertion cathodes.[9]

Therefore, transition metal oxides that include lithium, such as $LiCoO_2$,[11] $LiNiO_2$,[12] $LiMn_2O_4$,[13] $LiFePO_4$ (ref. 14) as well as their modified forms, have been extensively researched to create effective cathode materials for LIBs.[15] However the layered and spinel oxides generally suffer from safety, stability or cost limitations making olivine type LFP an attractive alternative. Due to its fast charging ability and lifespan consistency, LFP is regarded as a potential cathode material.[16] The capability for rapid charging is increasingly regarded as a crucial feature in the advancement of rechargeable energy storage systems, particularly within the realm of electric vehicles

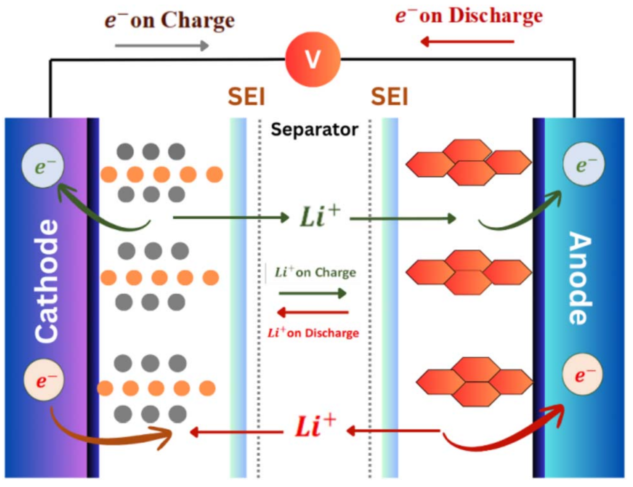

Fig. 1 Schematic of working principle of lithium ion battery during charge and discharge.

---

[a] Department of Physics, University of Gujrat, Gujrat 50700, Pakistan. E-mail: abdulmajid40@yahoo.com
[b] Department of Chemistry, University of Gujrat, Gujrat 50700, Pakistan
[c] Mechanical and Industrial Engineering Department, Abu Dhabi University, Abu Dhabi 59911, United Arab Emirates
[d] Department of Physics, Faculty of Science, Firat University, 23119 Elazig, Turkey

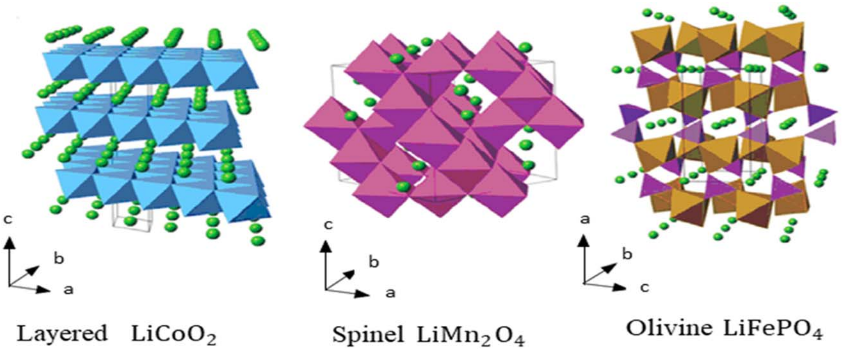

Fig. 2 Crystal structures of layered $LiCoO_2$, spinel $LiMn_2O_4$ and olivine $LiFePO_4$ cathode materials.[9,10] Reproduced from open access article ref. 9 with permission MDPI, copyright 2014.

(EVs).[17] LFP is identified as a pivotal cathode material due to its superior thermal stability, prolonged cycle life, economical, non-hazardous, and reliable performance under high-temperature conditions.[16,18,19] Owing to its crystalline structure in bulk and optimum particle size in nanostructure, LFP has a greater charge storage capacity of approximately 170 mAh g^{-1}, enabling good performance even at high discharge rates.[20] Nevertheless, its rate capability is hindered by its intrinsically poor electronic/ionic conductivities and weak lithium-ion mobility, low bulk density, which limits its practical applications.[21–25] The low-rate capability of LFP makes it extremely difficult to be widely sold as a cathodic active material for LIBs.[23] Techniques including particle downsizing, morphological control, cation doping and surface coating have been extensively used to overcome these limitations.[26–30] Although doping improves conductivity, its mechanism remains debated, while particle shrinking enhances Li^+ ion transport, it also increases surface area which results in reduced bulk density and increased polarization.[31–33] One of the most successful approach for improving the electrical mobility and electrochemical stability of LFP is surface coating.[34] Although carbon coating has significantly improved the electron transport of LFP, further advancements in charge–discharge performance are being understood through synergistic strategies, including heteroatom doping (*e.g.*, nitrogen and magnesium) metal oxide or nanoscale surface modification and the incorporation of conductive frameworks such as multi-walled carbon nanotubes (MWCNTs).[35–38] Beyond enhancing conductivity and stability, these modification techniques are pivotal in overcoming challenges related to scalability and commercialization, ensuring that laboratory improvements can be effectively implemented on a larger scale.[39] Recent reports also emphasize the effectiveness of such advanced strategies in improving LFP performance and scalability.[40,41] Building on these advances, LFP can also be used with sulfide and composite solid electrolyte which has been demonstrated to improve thermal stability, interfacial stability and ionic conductivity.[5] These configurations also enables *in situ* interface chemistry, polymer electrolytes, stable mixed conducting interface and uniform lithium ion deposition for all next generation solid state batteries.[39–44]

2. Cathode modification

The primary drawback of $LiFePO_4$ with PO_4^{3-} polyanions is its inherently low electrical conductivity, which leads to significant polarization during both charging and discharging processes. If its conductive agent is not well distributed, the total capacity of LFP is generally diminished. Additionally, the instability of the electrolyte contributes to a decline in performance. $LiPF_6$, one of the most widely used lithium salts in LIB, is extremely sensitive to moisture, even at very low concentrations. The hydrolysis reaction model of $LiPF_6$ in the battery electrolyte are represented as.[45–47]

$$LiPF_6 \leftrightharpoons LiF + PF_5 \tag{1}$$

$$PF_5 + H_2O \rightarrow 2HF + POF_3 \tag{2}$$

The HF produced in this reaction attacks the LFP surface, $LiPF_6$ can dissolve transition metals and damage the cathode surface. To address these challenges, surface coatings are used as an effective solution.[46] Conclusively, the electrochemical stability of LIBs is enhanced, and acidity is mitigated by incorporating nanosized oxide particles into the electrolyte to absorb HF. Additionally, oxide nanoparticles applied to the cathode surface can locally absorb HF, thereby reducing the acidic environment near the cathode and protects the active material.[41,48,49]

Surface coatings offer several advantages for LFP based cathodes:

(i) Forming an electronically conductive layer that facilitates charge transfer.

(ii) Modifying the surface to improve electrochemical performance and structural stability.

(iii) Functioning as HF scavengers, which decrease electrolyte acidity and shield the cathode from dissolution.[50]

For example, ZnO and Al_2O_3 coating layers can react with HF to create stable molecules like ZnF_2 and AlF_3, which lowers the acid concentration and enhances battery efficiency.[51,52]

$$ZnO + 2HF \rightarrow ZnF_2 + H_2O \tag{3}$$

$$Al_2O_3 + 6HF \rightarrow 2AlF_3 + 3H_2O \tag{4}$$

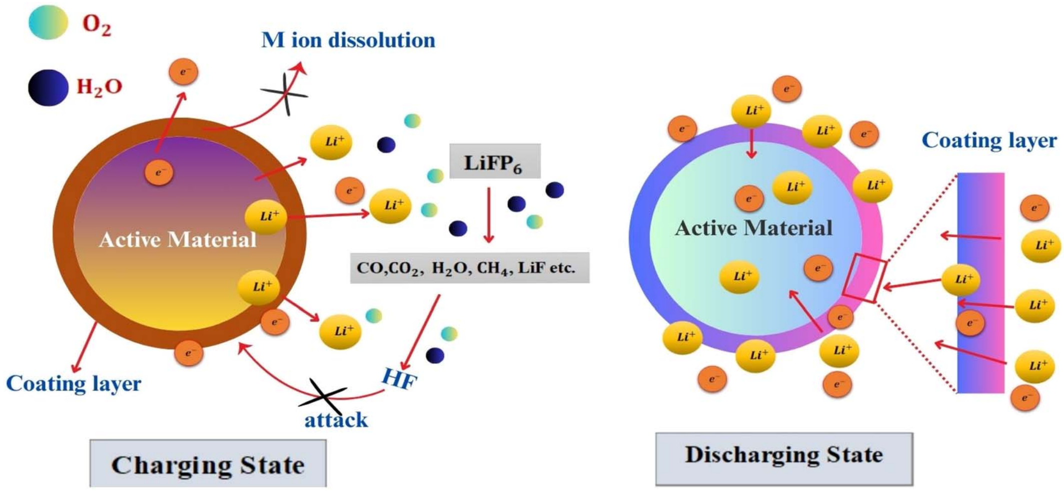

Fig. 3 Effect of surface coating on cathode materials in suppressing side reactions and enhancing structural stability.

These reactions produce protective layers that slow down cathode degradation and improve short term capacity retention. However over long cycling periods, HF scavenger depletes, highlighting the importance of nanoscale coatings with high chemical stability.[53] The protective layer maintains the material robustness of the cathode by creating a barrier that reduces undesirable interactions between the electrode and electrolyte (Fig. 3).[54]

3. Synthesis techniques for LFP-based cathodes

Cathode-based materials such as LFP can be created in several ways, including carbon-based reduction, microwave reactions, hydrothermal, and sol–gel methods, which are described below.

3.1 Hydrothermal approach

Hydrothermal synthesis is an effective way for formulating fine particles, providing benefits such as a simple procedure and short energy consumption; unfortunately, the plank-like geometries of the $LiFePO_4$ powders produced *via* this approach can have negative impacts on the material's chemical and physical characteristics, and by adding PEG (polyethylene glycol) to the original solvent mixture, well-crystallized $LiFePO_4$ particles were obtained using a hydrothermal technique; consequently, a starting capacity of 143 mAh g^{-1} was attained.[55]

A microwave assisted hydrothermal approach was used to quickly synthesize LFP at 200 °C in 10 minutes, producing a high purity single phase material without the need of post calcination. The cathode showed a specific of 126 mAh g^{-1} at 0.1C and a coulombic efficiency of 94–96%, highlighting this route as a fast and energy efficient process for LFP preparation.[56] The hydrothermal synthesis of LFP involved the use of urea as a reducing agent, at different temperatures (150–200 °C), and Li precursors (LiCl, $LiNO_3$, LiOH, and Li_2SO_4). Single-phase LFP forms were characterized using a dissolution–precipitation mechanism at temperatures between 170 and 180 °C and reaction periods greater than 12 hours, conclusively, Li_2SO_4 produced flower-like agglomerates, while the other precursors produced bulky particles (Fig. 4).[57]

The amalgamation of $LiFePO_4$ involved varying the ratio of LiOH to H_3PO_4, maintaining the acidic or basic nature of the solution at 6.5, and mixing the liquid at a controlled temperature to guarantee homogeneity. The combination was subsequently hydrothermally treated for 12 hours at 180 °C.[5,58] A hydrothermal approach was used for $LiFePO_4$ having doped and undoped Mg, as a result, doping imposes minor impact on the $LiFePO_4$ composites electrochemical performance and electronic conductivity.[59] Phospho-olivine LFP cathode-based materials were effectively organized through hydrothermal

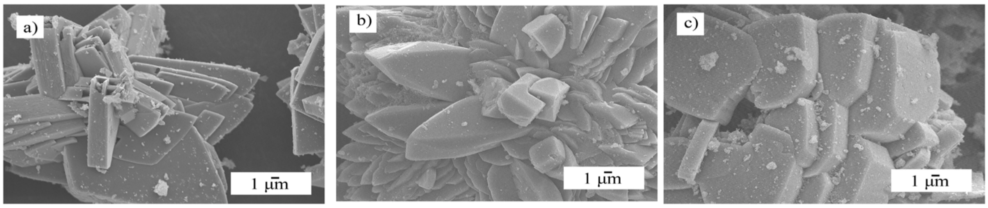

Fig. 4 FE-SEM micrographs of LFP powders prepared hydrothermally for 12 h with 20 mmol urea and Li_2SO_4 (Li : Fe : P = 3 : 1 : 1) at different temperatures: 170 °C (a), 180 °C (b), 190 °C (c).[57] This figure is adopted/reproduced/reprinted from ref. 57 with agreement from Elsevier, copyright 2017.

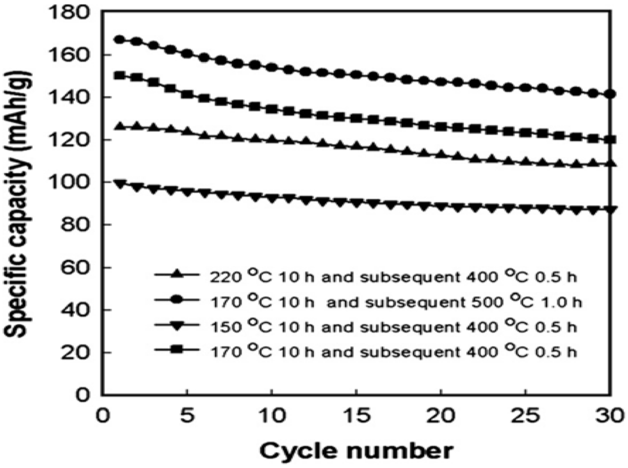

Fig. 5 Cycling stability of $LiFePO_4$ prepared at different temperatures.[60] This figure is adopted/reproduced/reprinted from ref. 60 with agreement from Elsevier, copyright 2007.

reactions at diverse temperatures. An orthorhombic olivine-type structure with a normal grain size of 200 nm was confirmed by XRD and SEM studies of the sample that was produced at 170 °C and then calcined at 500 °C (Fig. 5), which represented 98% of the hypothetical capacity and had the maximum output storage capacity of 167 mAh g^{-1} at 0.1C.[60]

3.2 Microwave-based method

Microwave processing technology is an innovative thermal treatment method that utilizes the effective absorption and transformation of electromagnetic radiation, and this approach is unique in that it uses a self-heating mechanism, which causes the sample to heat rapidly and continuously inside, frequently at much lower temperatures than with traditional heating techniques.[61]

$LiFePO_4$ nanorods were rapidly created below 300 °C utilizing microwave-based techniques (microwave solvothermal/hydrothermal), and conductivity was enhanced by carbon coating (*in situ* with glucose, *ex situ* with sucrose); also, better battery performance was demonstrated by smaller particles from the MW-ST(microwave solvothermal) technique because of improved electrical conductivity and lithium ions mobility.[62] The $LiFePO_4$–C composite was prepared quickly and easily by ball-milling for thirty minutes and then heating it in a microwave for 2–4 minutes. The material displayed fine, homogeneous particle size, equal carbon distribution, and was well-crystallized and free of Fe^{3+} impurities, this material provided an early-stage discharge capacity of 161 mAh g^{-1} and showed extraordinary long-term stability at C/10 (Fig. 6).[63]

The effective amalgamation of $LiFePO_4$ involves simple microwave heating without the use of reductive gas flow. By using activated carbon as the microwave absorber, the heat treatment time can be significantly reduced, and the need for any precursor can be eliminated, as it is not a precursor itself. In addition, this procedure is extremely simple, inexpensive, and repeatable. Consequently, we achieved the maximal discharge specific capacity and the optimal stability during cycling at a duration of four minutes of microwave heating.[64]

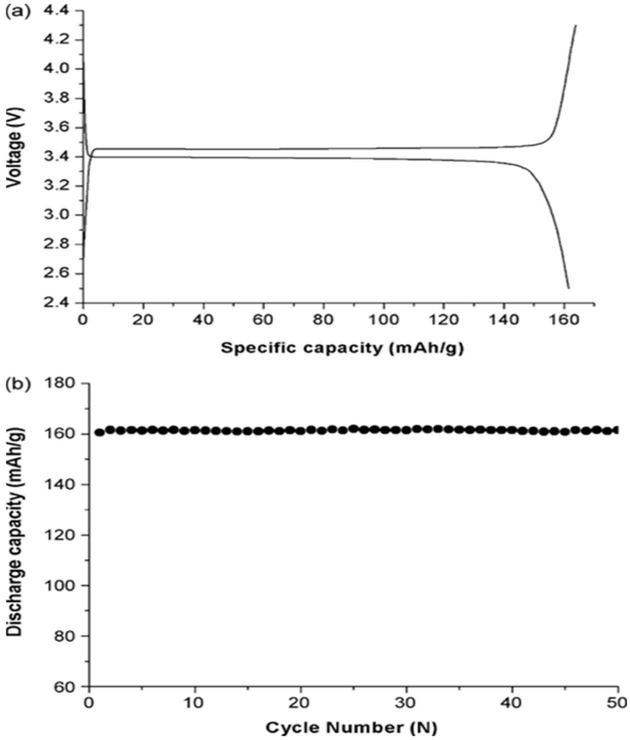

Fig. 6 (a) Charge–discharge curve and (b) cycling performance of $LiFePO_4$/C (8.10 : 1 ball milling, 2 min microwave) at 27 °C.[63] This figure isadopted/reproduced/reprinted from ref. 63 with permission from Elsevier, copyright 2007.

Subsequently, a 4-minute microwave heating (Fig. 7), which can be charged with 159 mAh g^{-1} and discharge with 151 mAh g^{-1} at room temperature, where the early discharge capacities at C/10, C/2, and 1C rates were 151 mAh g^{-1},139 mAh g^{-1} and 134

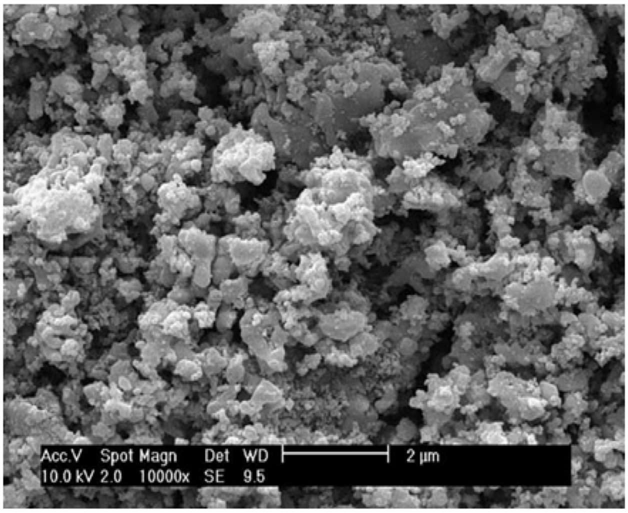

Fig. 7 SEM Analysis of $LiFePO_4$ particles synthesized by microwave heating for 4 minutes.[64] This figure is adopted/reproduced/reprinted from ref. 64 with permission from Elsevier, copyright 2003.

mAh g^{-1} respectively, showing good cycle life properties and rate capabilities.[64]

Using microwave processing, LFP with high selective capacity is made from the precursor $NH_4FePO_4 \cdot H_2O$ showing a two-phase charging/discharging behavior, maintaining a uniform potential around 3.4 V, and as the heating time increases, the discharge capacity improves, specimen A gives 119 mAh g^{-1}, specimen B (10 min) 134 mAh g^{-1}, specimen C (15 min) 156 mAh g^{-1} while overheated specimen D drops to 102 mAh g^{-1}, which indicates that these samples are stable over time, however, specimen C performed best even at high current. This implies that 15 minutes of heating provides the best battery performance, even though specimen D has higher conductivity.[65]

3.3 Carbon-based reduction approach

An economical and environmentally responsible approach for producing LFP/C powders is the carbothermal reduction procedure, which provides precise control over particle morphology and oxidation states, improving surface area, electron transport, and lithium-ion diffusion. A consistent sheet of carbon is created on the particle surface by heating the carbon source with the precursor, greatly enhancing the electrical conductivity and electrochemical performance.[5]

Wet milling and spray drying carbothermal reduction (WSC) have been used to form a new mesoporous bowl-shaped LFP/C composite. This composite is characterized by pores approximately 13.3 nm in size, an effective area of 29.4 m^2 g^{-1}, and primary particles uniformly coated with carbon, each measuring less than 100 nm. It shows a greater storage capacity of approximately 123 mAh g^{-1} at 10C, maintaining this capacity over 100 cycles without degradation. The exceptional rate performance of this composite is ascribed to enhanced lithium-ion distribution, an expanded reaction surface area, and improved electronic conductivity (Fig. 8).[66]

Using β-FeOOH nanorods as the initial precursor and glucose as the carbon donor and reducer, a thermal reduction method was used to create the LFP/C composite. The findings indicate that the electrochemical performance of the final LFP/C product is influenced by the amount of carbon and morphology of the starting material. The LFP14 specimen containing 2.79 wt% carbon, exhibited discharge capacities of 158.8, 144.3, 111.0, and 92.9 mAh g^{-1} at 0.1, 1, 10, and 15C rates, respectively, and regained 157.5 mAh g^{-1} or 99.2% of its original capacity when the rate was returned from 15C to 0.1C. This highlights that the LFP/C material synthesized by this method offers strong potential for large-scale production and application in LIBs, especially for electric and hybrid vehicles, owing to its excellent cycling durability and negligible drop of capacity after 100 cycles at 0.5C.[67]

3.4 Sol–gel approach

The sol–gel process was used to control the powder's grain size and improve its electrochemical characteristics. The adipic acid-assisted sol–gel technique was created at 670 °C in an argon environment. There were a few large particles, approximately 200–300 nm in size, mixed with a large number of polycrystalline particles, approximately 50–100 nm in size. At a high current density of more than 30C, the cell showed a high initial discharge capacity beyond 150 mAh g^{-1} and good cycle performance.[68] The sol–gel method was successfully used to create a pure and highly crystalline form of LFP with regulated levels of LiI (lithium Iodide) and carbon covering. LFP's purity and particle size of LFP were significantly affected by the amount of LiI. During cycling, the optimized LFP sample displayed a steady current density and a discharge capacity that was nearly equal to its theoretical value. Also, by creating a cavity-like structure, this carbon coating improved the diffusion and charge transfer of lithium ions.[69] In the sol–gel procedure, citric acid was utilized as a carbon precursor to produce both pure LFP and LFP/C. The creation of LFP/C involved the employment of three dissimilar metals to citric acid stoichiometries specifically 1 : 0.5, 1 : 1, and 1 : 2. Among the four samples that were prepared, the consequences showed that LFP/C (1 : 1) had the highest discharge capacity, measuring 148.2 mAh g^{-1} at a rate of 0.1C and 113.1 mAh g^{-1} at a high rate of 5C. This was due to its ideal thickness of 4.2 nm and increased graphene-like carbon layer and beyond 300 cycles at a 1C rate, the sample LFP/C (1 : 1) exhibits 96% capacity stability.[70] LFP/C sample was synthesized with good performance by a bio-

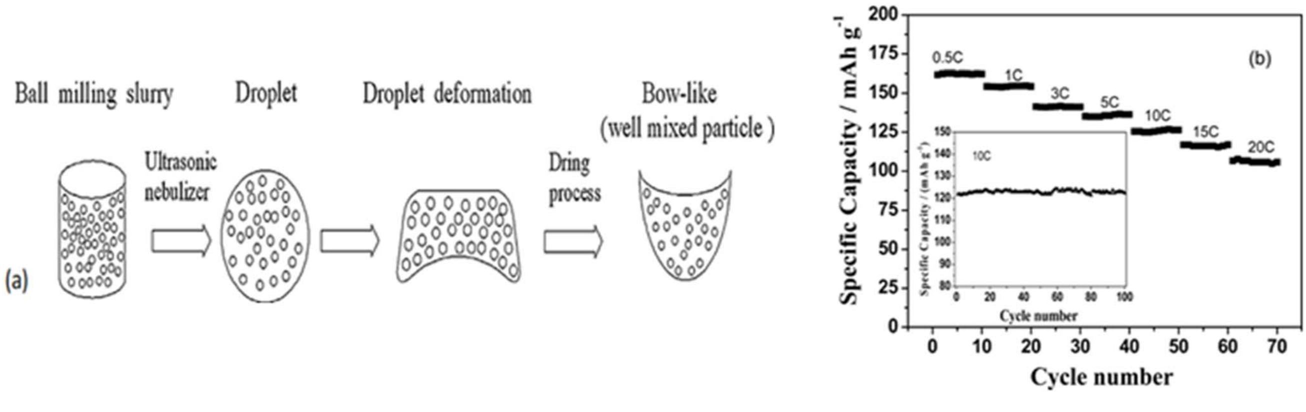

Fig. 8 (a) Formation scheme of the mesoporous bowl-like $LiFePO_4$/C morphology and (b) its discharge profiles and rate capability at different current densities.[66] This figure being adopted/reproduced/reprinted from ref. 66 with permission from Elsevier, copyright 2003.

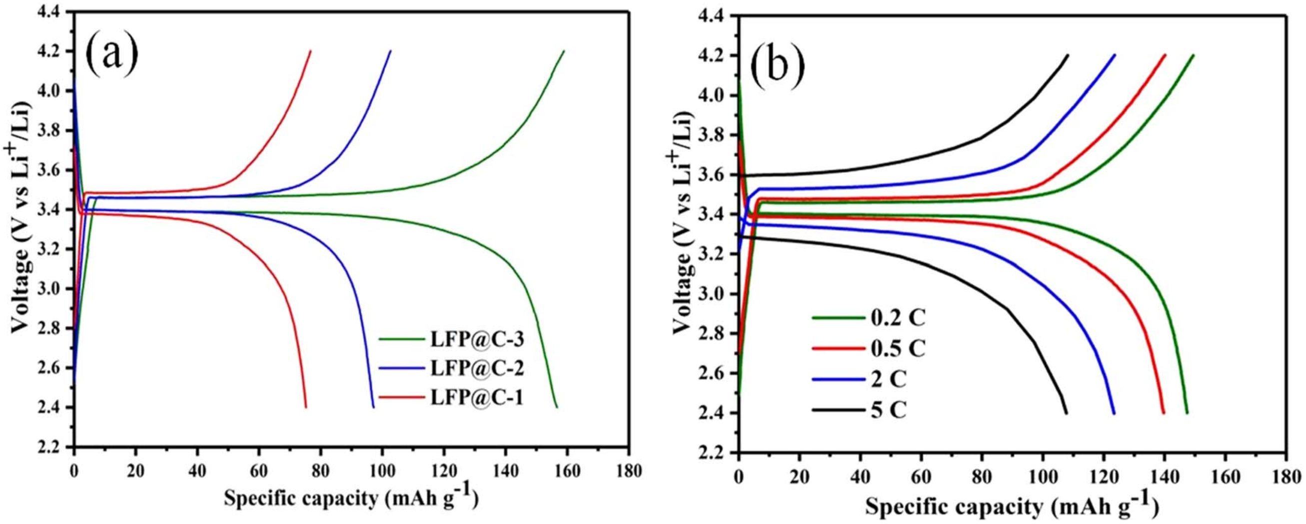

Fig. 9 (a) Initial charge–discharge profiles of synthesized electrode materials at 0.1C and (b) charge–discharge profile of LFP@C-3 at different rates of 0.2C, 0.5C, 2C and 5C.[72] This figure is reproduced from ref. 72 with the permission from Elsevier, copyright 2019.

synthetic sol–gel process that used yeast as a bio carbon source. The sample annealed at 800 °C had the best retention (94.3 mAh g^{-1} at 5C after 100 cycles) and superior discharge capacity (158.3 mAh g^{-1} at 0.1C) demonstrating its outstanding potential as a high performance cathode material.[71] Using a citric acid as a chelating agent and yeast as a template carbon coated LFP samples (LFP@C-1, LFP@C-2, LFP@C-3) were synthesized in a bio assisted sol–gel procedure (Table 1). Among them, LFP@C-3 exhibited the highest discharge capacity (~157 mAh g^{-1} at 0.1C) and best rate performance because of its superior electron transport, higher purity and homogeneous carbon coating (Fig. 9).[72]

4. Surface degradation and protection mechanism

A well-known and effective technique for safeguarding cathode materials while enhancing lithium-ion surface coating's specific capacity, thermal stability, and electrochemical performance is surface covering. Carbonaceous compounds like reduced graphene oxide (rGO), carbon nanotubes (CNTs), graphene, porous carbon, and graphene are the most commonly utilized covering materials (Fig. 10) because of the following benefits: (1) having excellent stability, both chemically and electrochemically. Carbon materials exhibit electrochemical activity at very low potentials, showing great electrochemical stability and strong defense against corrosion of acid electrolytes, owing to interactions between the electrode and electrolyte. Furthermore, carbon compounds can shield the cathode material from atmospheric oxygen and moisture because they are difficult to oxidize. (2) In addition, carbon has special physical characteristics such as low density, great mechanical strength, structural flexibility, and anisotropic conductivity.[81,82] (3) High electrical conductivity. Carbon is a valuable covering material because it is an excellent conductor of electricity. (4) Cost effectiveness. Carbon is readily available, inexpensive, and friendly material.

Table 1 Merits and demerits of different approaches for making LFP cathode active material

Preparation method	Merits	Demerits
Hydrothermal method	Superior performance (including exceptional rate capabilities (120 mAh g^{-1} at 10C) and high reversible capacity (up to 163.6 mAh g^{-1}))[73]	Requires expensive lithium salt[73]
	Material stability and reduced costs of production[74]	High-pressure equipment may be needed and rong reaction times[76]
	Low energy consumption[75]	
Microwave-based method	Efficient heating and brief synthesis duration shorter processing duration[77]	Energy consumption. Temperature measurement limitations[79]
	Eco-friendliness[78]	
Carbon reduction method	Simple procedure, low cost of manufacturing and low cost of raw materials[5]	Stability is difficult to maintain. Mixing is homogeneous, and oxidation problems during drying are common[5]
Sol–gel method	Good control of particle size, increased surface area and enhanced electrochemical properties performance[71]	Challenges in scaling and temperature control[80]

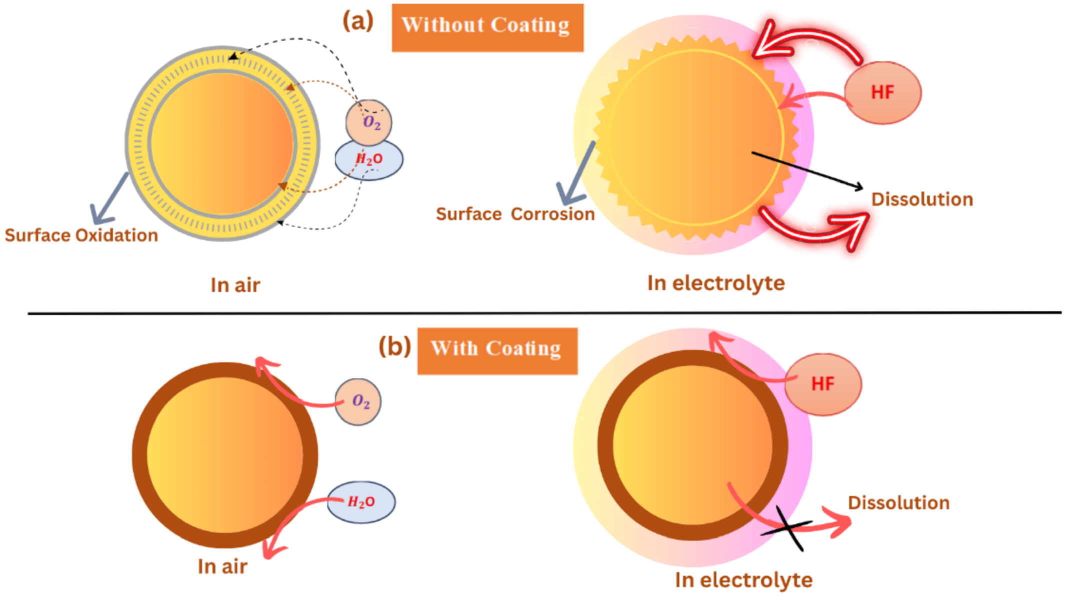

Fig. 10 Schematic illustration of cathode behavior with (b) and without carbon coating (a).

Additionally, by modifying the carbon material and preparation conditions, the thickness and conductivity of the carbon covering can be adjusted.[21] Owing to its superior qualities, carbon is frequently considered a good surface-coating material for LIB cathodes. Improving superficial chemical stability, increasing the material's structural stability, and facilitating effective lithium-ion diffusion are the three main advantages of carbon coating. Each of these mechanisms supports and strengthens the other. The carbon layer strengthens the interfacial chemical stability and permits more uniform lithium-ion transport during charge–discharge cycles by reducing the dissolution of transition metal ions and surface imperfections.[81,83]

5. Performance enhancement approaches of LFP cathodes

5.1 Carbon-based coating for LFP

Conductive materials, namely amorphous carbon, natural graphite, and fibrous carbon, are combined with electrode components to improve electrical pathways since high-rate battery charging and discharging depend on well-organized electron and lithium-ion transfer. However, when the LFP particle size is reduced to the nano or submicron level, more carbon is required to connect the particles, reducing the amount of active substance and thus affecting the energy per unit mass. Challenges, such as achieving uniform carbon distribution, remain, which can be addressed through mechanofusion coating and surfactant-assisted slurry preparation or by combining active compounds with carbon during synthesis to improve conductivity.[84]

Carbonized LFP and LFP/C composites were made with a variety of LFP precursors and carbon sources, such as stearic acid,[85] sucrose, glucose, sugar,[86] and resorcinol–formaldehyde.[87] The synthesis required heat treatment in an inert environment at temperatures between 500 °C and 800 °C.[21] The LFP crystal particles were maintained between 100 and 200 nm in size, and their mass percentage of carbon ranged from 3 to 15%. These materials exhibited outstanding cycle and rate capabilities, as well as a 160 mAh g^{-1} discharge capacity, demonstrating good electrochemical performance. But even a tiny quantity of carbon (less than 1% mass) was shown to drastically lower the final electrode sheet's density.[88] When the carbon concentration reached 31 wt%, the electrical conductivity of the electrode sheet improved by approximately seven orders of magnitude, demonstrating the effectiveness of carbon-coated LFP with sucrose.[89] The performance was also improved by the covered layer depth and homogeneity of the carbon covering, as demonstrated by the improved outcomes when more carbon was applied to the carbon-coated LFP particles.[90] Carbonized LFP was prepared hydrothermally with glucose as the carbon precursor; the resultant rod-like LFP particles were uniformly sized at about 220 nm, and they were covered in a layer of carbon that was 5–12 nm thick and containing 5 wt% carbon. Excellent cycling and rate performance were demonstrated by these particles.[21,91]

5.2 MWCNT-based conductive coatings

CNTs are ideal for nanoscale molecular devices because of their small size, great tensile strength, chemical durability, high thermal conductivity, strong sp^2 carbon bonds, and special electrical characteristics.[92]

Later, the insertion of MWCNTs into the carbon coating, their high aspect ratio, three-dimensional structure, and superior electron mobility created a robust conductive network and increased the mechanical strength.[93,94] LFP covered with MWCNTs was synthesized *via* hydrothermal approach, and then subjected to heat treatment. Various characterizations

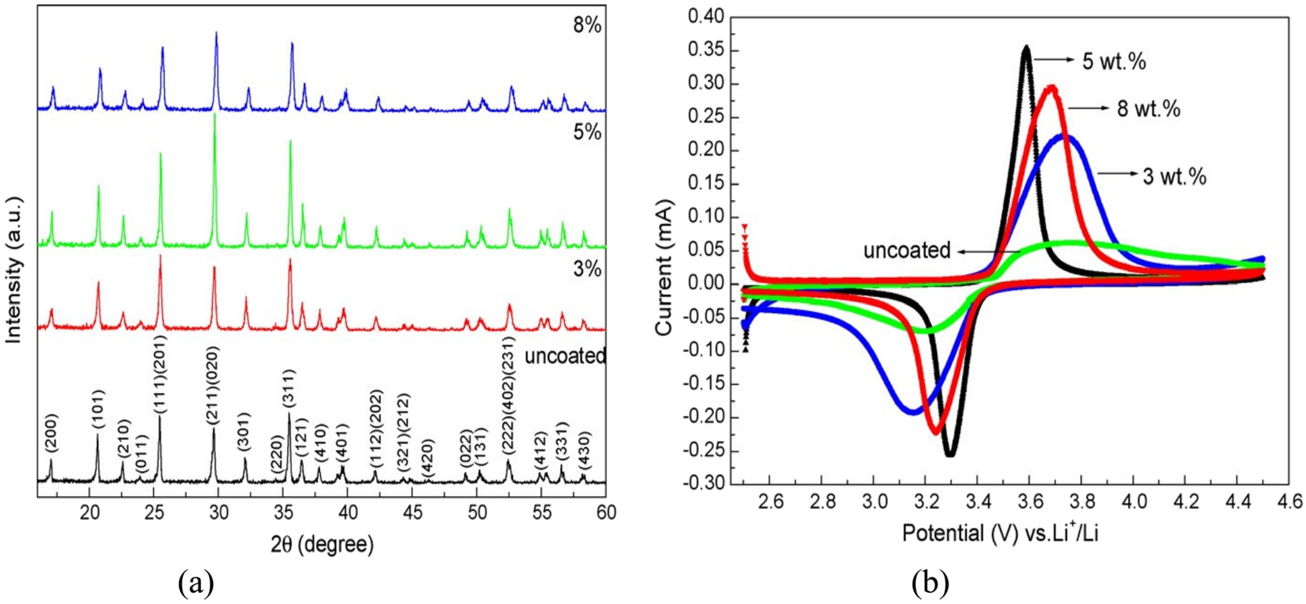

Fig. 11 Comparison of the XRD patterns (a) and cyclic voltammetry profiles (b) of the uncoated LFP and LFP/MWCNT composites.[95] Both figures (a and b) are reproduced from ref. 95 with permission from Elsevier, copyright 2009.

were performed to examine the pure LFP and LFP-MWCNT samples, as shown in Fig. 11a and b.[95]

The LFP-MWCNTs exhibited a superior discharge performance and improved cycling durability in contrast to pristine LFP. Notably, the sample containing 5 wt% MWCNTs demonstrated an initial discharge capacity of 160.3 mAh g^{-1} at 0.3C, with only 0.4% capacity fading observed upon 50 cycles.[95]

The effectiveness of applying MWCNTs was tested using three different types of LFP cathode samples: mechano-fusion (MF) dry coating, conventional coating, and the new incipient coating (IC) approach (Fig. 12). The IC technique created a uniform and thin coating layer with minimal material, improving electronic and ionic conduction, lowering internal resistance, and suppresses particle aggregation. As a result, the rate capacity increased by 30% and had a capacity of 157.57 mAh g^{-1} at 0.1C, as well as outstanding, long-lasting cycling durability, preserving 99.33% of its capacity after 150 cycles at 1C/45 °C.[96]

A nanosized C/LFP/MWCNTs composite produced by hydrothermal and electro polymerization techniques demonstrated outstanding electrochemical performance, delivering 169.9 mAh g^{-1} at C/10 and 143.4 mAh g^{-1} at 20 C. After 200 cycles, the formation of a 3D conductive network improved the transportation of both electrons and Li^+ ions, resulting in >95% capacity retention.[97]

5.3 Heteroatom doping in carbon layers

Heteroatom doping in carbon layers has been a successful method for improving LFP cathode electrochemical behavior.[98] Heteroatoms like N, S, B, P, and F can be added to the carbon network to enhance electrochemical performance by promoting the diffusion of lithium ions, generating defect sites, and

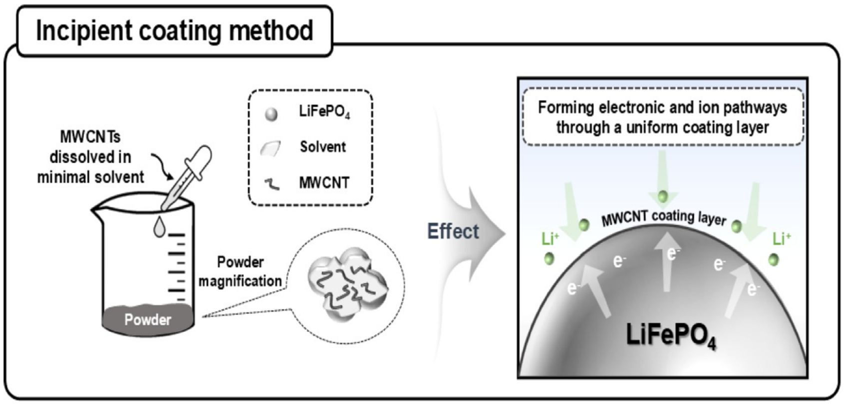

Fig. 12 Incipient coating of MWCNTs on LFP enhances electron and ion pathways.[96] Reproduced from ref. 96 with permission from the American Chemical Society, copyright 2025.

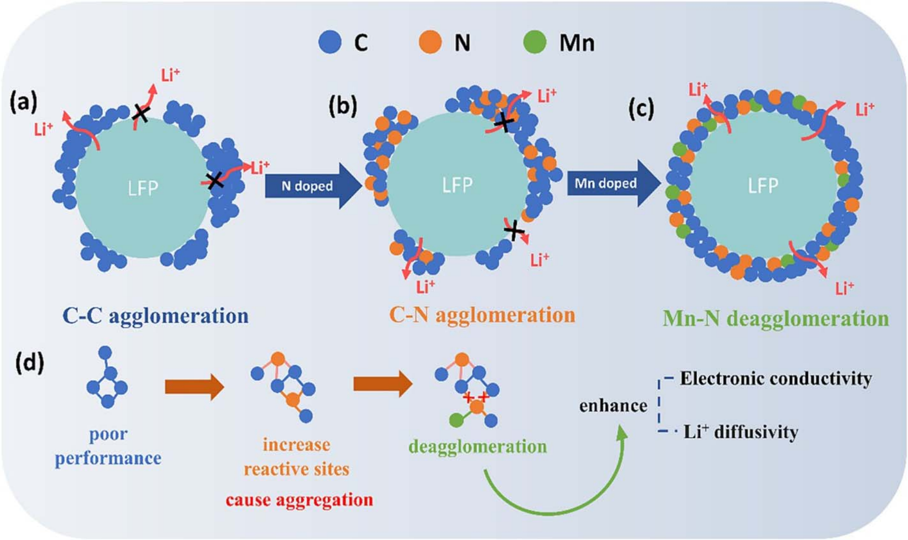

Fig. 13 (a) Carbon coating on LFP; (b) layer of N-doped carbon on LFP; (c) N–Mn co-doped carbon layer on LFP; and (d) Mn-induced deagglomeration effect.[38] Reproduced from ref. 38 with permission from the American Chemical Society, copyright 2024.

boosting electronic conductivity.[99] LFP-based cathodes in LIBs are made more electrochemically efficient by nitrogen-doped carbon surface engineering.[38,100–102] N (nitrogen) doping improves electron transport by boosting carrier density, enhancing the interface between carbon and LFP, and forming active sites and surface defects that reduce the energy barrier to

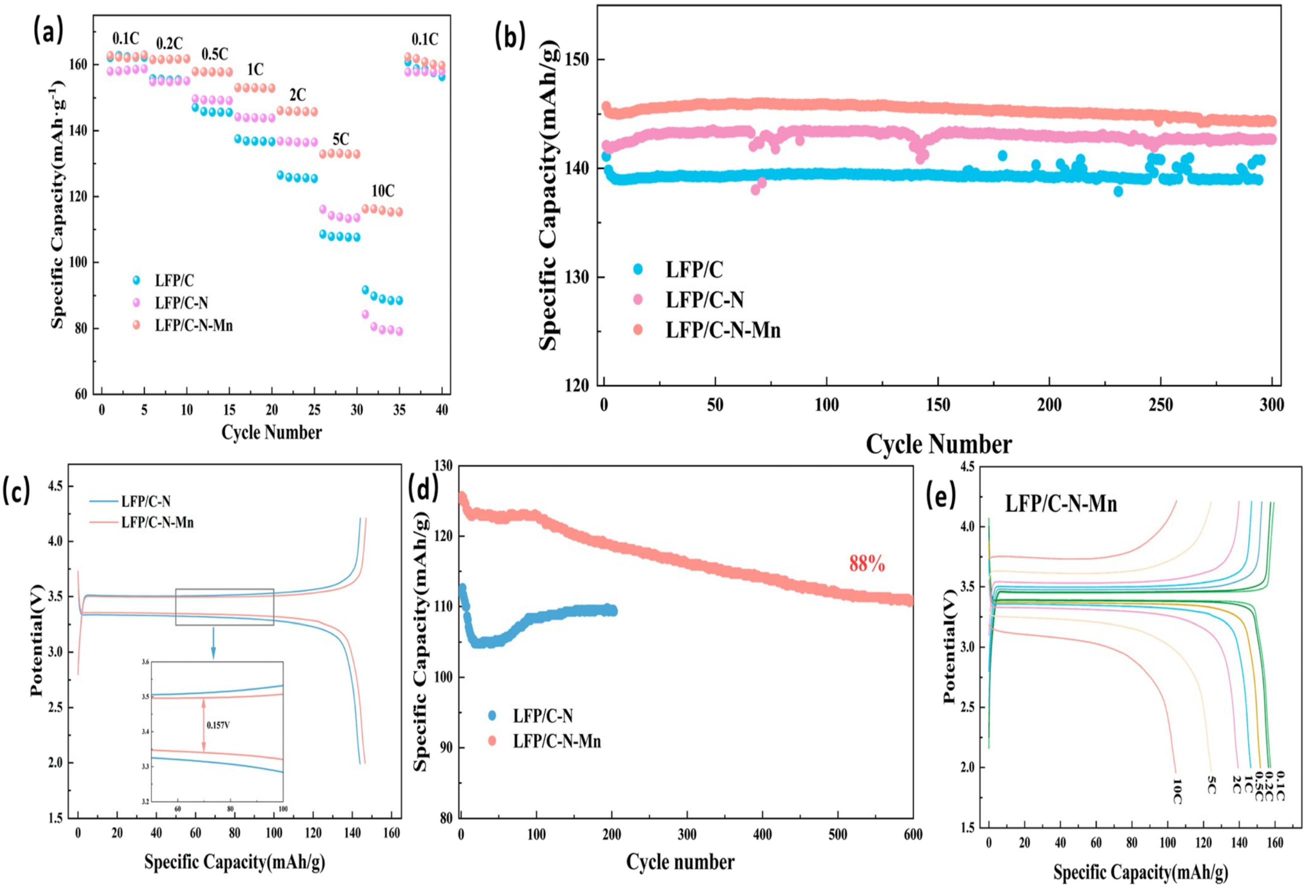

Fig. 14 Electrochemical performance of LFP composites: (a) rate performance (0.1–10C); (b) cycling stability at 1C; (c) charge/discharge shapes with voltage plateau inset; (d) cycling at 5C, and (e) charge/discharge profiles of LFP/C–N–Mn (0.1–10C).[38] Reproduced from ref. 38 with permission from the American Chemical Society, copyright 2024.

ion penetration.[101,103] However, excessive nitrogen doping frequently results in the production of thick C–N domains, creating agglomeration in the coating layer and poor high-rate performance. This may be efficiently addressed by utilizing a synergistic doping method that includes both nitrogen and manganese(Mn).[38] Dual doping with Mn and N (Fig. 13) increases the ductility of LFP by decreasing microcrack development and minimizing shear deformation, which lessens the barricade of lithium ion transport, promoting quicker ion transport and overall electrochemical performance.[104] For LFP particles at the micrometer scale, the LFP/C–N–Mn material demonstrated extraordinary rate capacity and robust cycling behavior (*e.g.*, 119 mAh g^{-1} at 10C, 88% retention after 600 cycles at 5C) (Fig. 14).[38]

Additionally, the beneficial effects of dual-heteroatom doping, such as N, S co-doping, create a large number of active sites and porous frameworks that improve Li storage and charge transport.[105] For instance, the solid state approach of synthesizing N,S doped carbon-coated LFP(NSC-@LFP) with methionine exhibits outstanding performance, providing 155 mAh g^{-1} at 0.1C and 99% capacity retention after 200 cycles due to better ionic/electronic conductivity and rapid ion diffusion.[99] LFP/C composites with F, Mn, Nb, and Mg dopants that were made by ball milling shown superior electrochemical performance were improved (Fig. 15). As a result, Nb enhanced cycling stability (>96% after 100 cycles), Mn increased low temperature capacity (113.7 mAh g^{-1} at 10C) demonstrating the beneficial effects of elemental doping for LFP/C cathodes.[98]

$LiFe_{0.98}M_{0.02}PO_4/C$ (M = Mg, Ni, Co, Sr) composites were created using a solid-state technique with glucose and Fe_2O_3 where XRD verified that there were no impurity phases present (Fig. 16), and doping caused changes in unit–cell parameters (Table 2), which led to an enlarged lattice volume that widened the Li^+ diffusion channels, improved charge–discharge behavior, and introduced lattice distortions that increased hole formation, which improved electronic conductivity (Table 3), among the dopants, Ni^{2+} demonstrated the uppermost conductivity (3.11×10^{-3} S m^{-1}) and excellent electrochemical performance, with an initial discharge capacity of 156.6 mAh g^{-1} at 0.2C and 149.4 mAh g^{-1} at 1C, respectively, maintaining 98.8% and 97.2% capacity retention after 30 cycles.[106]

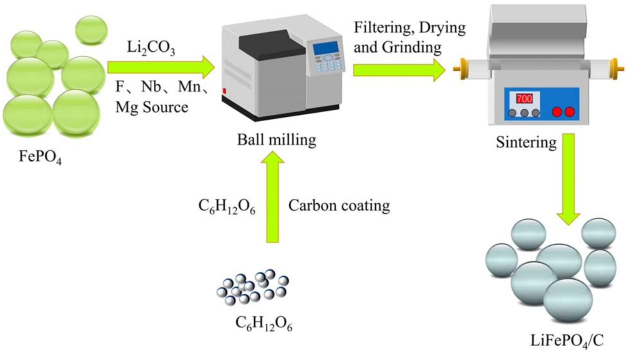

Fig. 15 Schematic representation of the carbothermal reduction process paired with a combined bulk phase doping approach to prepare LFP/C cathode materials.[98] Reproduced from open access article ref. 98 with permission MDPI,copyright 2024.

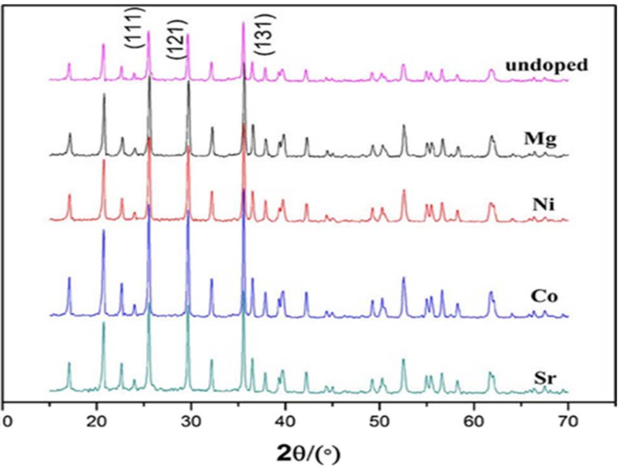

Fig. 16 XRD patterns of LFP samples doped with different metal ions.[106] Reproduced from ref. 106 with permission from the John Wiley and Sons, copyright 2013.

Table 2 Features of unit–cells in samples with different dopants.[106] Reproduced from ref. 106 with permission from the John Wiley and Sons, copyright 2013

Dopant	*a*/nm	*b*/nm	*c*/nm	*V*/nm^3
Undoped	1.0315	0.5962	0.4635	0.2851
Mg^{2+}	1.0317	0.5999	0.4693	0.2905
Ni^{2+}	1.0334	0.6007	0.4697	0.2916
Co^{2+}	1.0331	0.6000	0.4702	0.2914
Sr^{2+}	1.0339	0.6009	0.4701	0.2920

Table 3 Electronic conductivities of samples with various dopants.[106] Reproduced from ref. 106 with permission from the John Wiley and Sons, copyright 2013

Dopant	*σ*/(S per m)
Fe^{2+}	5.07×10^{-6}
Mg^{2+}	7.75×10^{-4}
Ni^{2+}	3.11×10^{-3}
Co^{2+}	8.63×10^{-4}
Sr^{2+}	1.68×10^{-5}

5.4 Metal oxide and nanosize coating

A variety of metal oxides, such as MgO,[107] ZnO,[108] Al_2O_3,[109] TiO_2,[110] ZrO_2,[111] and SiO_2 (ref. 112) are used to modify the surface of LFP based cathode materials.[113] Stabilization is essential for preserving the battery's integrity and performance over long cycles, and coatings decrease structural degradation and active lithium loss, which are two prominent attenuation mechanisms in LFP batteries.[114] It is believed that aluminum oxide (Al_2O_3) serve as one of the greatest suitable covering substances for improving the cathode materials' rate capabilities as well as capacity retention in LIBs.[109,115] By blocking

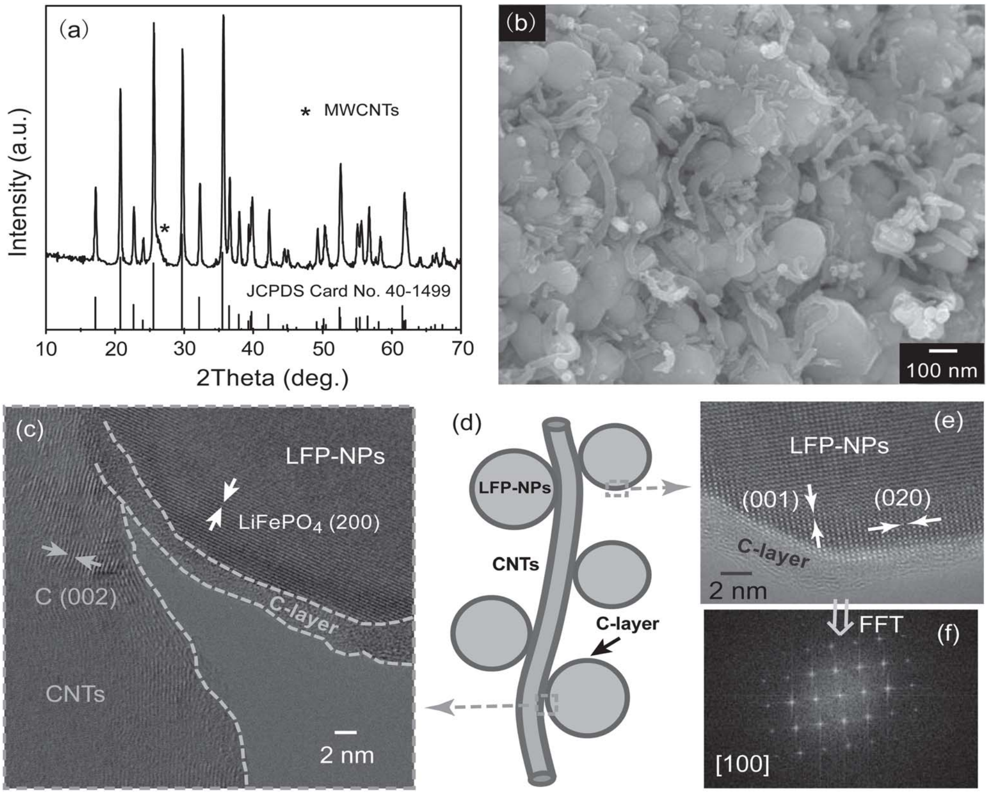

Fig. 17 (a) XRD pattern, (b) SEM, (c and e) HRTEM images, (d) schematic illustration of the generated LFP@C/CNT nanocomposite, and (f) the corresponding FFT from the HRTEM in (e).[122] Reproduced from ref. 122 with permission from John Wiley and Sons, copyright 2013.

straight interaction between the electrolyte and the cathode, the Al_2O_3 covering not only creates a protective CEI (cathode electrolyte interface) layer that lowers irreversible capacity loss and lithium-ion migration resistance, but it also neutralizes HF, safeguarding the electrode and stabilizing the cathode material's bulk structure.[116] The wide bandgap (3.7 eV) of amorphous Al_2O_3 (ref. 117) limits lithium-ion transport and leads to high interfacial resistance and overpotential at the CEI.[118,119] However, when applied as extremely thin nano-layers *via* atomic layer deposition (ALD), these limitations are reduced as the nanoscale thickness and grain boundaries facilitate lithium-ion migration.[120] The surface of LFP was covered with a uniform Al_2O_3 nano-coating of about 5–6 nm without altering its bulk framework, as confirmed through X-ray photoelectron spectroscopy (XPS) analysis, and this stable coating remained intact even after 300 charge/discharge cycles, greatly improving capacity retention and rate capability at high cycling rates like 10C.[36] Al_2O_3 coating does not vary the olivine framework of LFP, as all frameworks (pristine LFP/C, 1 LFP/C/Al_2O_3 and 2 LFP/C/Al_2O_3) shows pure phase with greater crystallinity.[36]

Using a chemical precipitation method, LFP/C composites were coated with MnO_2, Al_2O_3 (ref. 109) and CuO, where XRD analysis confirmed that the olivine structure remained intact, and electrochemical tests showed substantial perfection in superior rate performance capability and cycling durability, among them, the MnO_2-coated sample achieved a specific discharge capacity of 118.5 mAh g^{-1} at 3C with 93.7% capacity sustainability after 250 cycles, outperforming the uncoated material (95.1 mAh g^{-1}).[121]

Graphitized CNTs were joined with an amorphous carbon coating to form a dual nano-carbon decorated LFP (LFP@C/CNT) nanocomposite. This is permissible for exceptional ultrafast charge/discharge performance (∼59% capacity retaining at 120 °C) and improved low-temperature capability (∼71.4% retaining at −25 °C).[5,122] With an approximate crystallite size of about 90 nm on average, the orthorhombic LFP exhibits high phase purity, as shown by the XRD patterns in Fig. 17a. HRTEM (Fig. 17c–e) displays distinct lattice fringes, demonstrating the single-crystalline nature of LFP, whereas SEM images (Fig. 17b) show a uniform particle distribution. Each LFP particle is enclosed in a uniform 2–3 nm amorphous carbon layer, and connecting CNTs form a 3D conductive network (Fig. 17d) that improves electron transport. The FFT pattern (Fig. 17f) confirms the high crystallinity and orientation of the nanoparticles.[5,122]

6. Conclusions

LFP is a robust and stable cathode material for LIBs, celebrated for its intrinsic thermal robustness and outstanding cycling longevity. Unfortunately, slow lithium-ion diffusion, poor electronic/ionic conductivities and low bulk density limit its full potential. This review has systematically shed light on the evolution of LFP synthesis and modification strategies. Initially, efforts to overcome LFP's intrinsic limitations primarily revolved around carbon coating, which effectively improved electronic pathways. More recent advancements, however, highlight a significant paradigm shift towards sophisticated modification techniques. The incorporation of heteroatom doping, multi-walled carbon nanotubes (MWCNTs), and various metal oxide or nanoscale coatings has demonstrably enhanced both the electronic conductivity and rate capability of LFP cathodes. These modern approaches represent a crucial step forward, moving beyond traditional surface treatments to more intricate material engineering. The improvement in synthesis methods, emphasizing structural control and scalability, and post-synthesis modification techniques underscores a clear trajectory towards optimizing LFP. The enhanced performance achieved through these innovative strategies firmly positions LFP as a leading candidate for modern, highly efficient energy storage technologies, capable of meeting the escalating demands for efficient and sustainable battery technologies. The future research activities are expected to focus on synergistic approaches combining advanced synthesis with multi-component modification to unlock even greater electrochemical performance and durability in LFP cathodes. Furthermore, the incorporation of LFP with emerging solid-state electrolyte systems presents a particularly promising avenue toward the development of ASSLBs, which may offer improved safety, increased energy density, and enhanced long-term stability. These all advancements highlight the potential of LFP for the development of next-generation ASSLBs technologies.

Author contributions

Sania Ishtiaq: conceptualization, methodology, investigation, writing original draft preparation, visualization. Abdul Majid: supervision, validation, writing – review and editing, funding acquisition. Abdul Qadeer: investigation, resources, data curation. Mohammad Alkhedher: methodology, formal analysis, validation. Niyazi Bulut: conceptualization, project administration, writing review and editing.

Conflicts of interest

The authors declare that they have no known competing financial interests or personal relationships that could have appeared to influence the work reported in this paper.

Data availability

There is no additional data associated with this article.

References

1 P. Zhou, *et al.*, Research on the performance improvement method for lithium-ion battery in high-power application scenarios, *Energies*, 2024, **17**(7), 1746.
2 M. Quarti, A. Bayer and W. G. Bessler, Trade-off between energy density and fast-charge capability of lithium-ion batteries: A model-based design study of cells with thick electrodes, *Electrochem. Sci. Adv.*, 2023, **3**(1), e2100161.
3 Q. Li, *et al.*, A 700 W h kg^{-1} rechargeable pouch type lithium battery, *Chin. Phys. Lett.*, 2023, **40**(4), 048201.
4 M. Chaudhary, *et al.*, Surface modification of cathode materials for energy storage devices: A review, *Surf. Coat. Technol.*, 2021, **412**, 127009.
5 T. Chen, M. Li and J. Bae, Recent advances in lithium iron phosphate battery technology: a comprehensive review, *Batteries*, 2024, **10**(12), 424.
6 D. E. Demirocak, S. S. Srinivasan and E. K. Stefanakos, A review on nanocomposite materials for rechargeable Li-ion batteries, *Appl. Sci.*, 2017, **7**(7), 731.
7 M. M. Thackeray, *et al.*, Lithium insertion into manganese spinels, *Mater. Res. Bull.*, 1983, **18**(4), 461–472.
8 A. K. Padhi, K. S. Nanjundaswamy and J. B. Goodenough, Phospho-olivines as positive-electrode materials for rechargeable lithium batteries, *J. Electrochem. Soc.*, 1997, **144**(4), 1188.
9 K. Ariyoshi, K. Nishimura and D. Kitagawa, Quantum Chemical Analysis of the Correlation between Electrode Potential and Redox Center of Li-Insertion Materials: Olivine, Layered and Spinel Structures, and Aqua-Complexes, *ChemElectroChem*, 2023, **10**(19), e202300333.
10 C. M. Julien, *et al.*, Comparative issues of cathode materials for Li-ion batteries, *Inorganics*, 2014, **2**(1), 132–154.
11 Z. Zhuang, *et al.*, Ultrahigh-voltage LiCoO2 at 4.7 V by interface stabilization and band structure modification, *Adv. Mater.*, 2023, **35**(22), 2212059.
12 L. Karger, *et al.*, From Li 2 NiO 3 to high-performance LiNiO 2 cathodes for application in Li-ion and all-solid-state batteries, *Chem. Commun.*, 2024, **60**(80), 11355–11358.
13 O. Nyamaa, *et al.*, Enhanced LiMn 2 O 4 cathode performance in lithium-ion batteries through synergistic cation and anion substitution, *Mater. Adv.*, 2024, **5**(7), 2872–2887.
14 S.-h. Kwak and Y. J. Park, Improving the performance of LiFePO4 cathodes with a sulfur-modified carbon layer, *Batteries*, 2024, **10**(10), 348.
15 M. Qi, *et al.*, Improved electrochemical performances of carbon-coated LiFePO4 microspheres for Li-ion battery cathode, *Mater. Res. Express*, 2019, **6**(11), 115520.
16 H. Zhou, *et al.*, Effect of fast charging on degradation and safety characteristics of lithium-ion batteries with LiFePO4 cathodes, *Appl. Energy*, 2025, **377**, 124465.
17 Y. Lu and T. Zhu, Status and prospects of lithium iron phosphate manufacturing in the lithium battery industry, *MRS Commun.*, 2024, **14**(5), 888–899.
18 T. Zhao, *et al.*, An overview on the life cycle of lithium iron phosphate: synthesis, modification, application, and recycling, *Chem. Eng. J.*, 2024, **485**, 149923.
19 C. Chen, H. Ma and Y. Wang, The Progress and Future Prospects of Lithium Iron Phosphate Cathode Materials, *Highlights Sci. Eng. Technol.*, 2022, **3**, 31–42.
20 C. M. Julien, X. Zhang and A. Mauger, Lithium Iron phosphate: olivine material for high power Li-ion batteries, *Res. Dev. Mater. Sci.*, 2017, **2**, 3–6.

21 M. Inagaki, Carbon coating for enhancing the functionalities of materials, *Carbon*, 2012, **50**(9), 3247–3266.

22 T. Xu, *et al.*, Secondary-structured LiFePO4 cathode with high tap density and reversible capacity, *Mater. Lett.*, 2020, **274**, 128006.

23 C. Shen, *et al.*, Facile fabrication of compact LiFePO4/C composite with excellent atomically-efficient for high-energy-density Li-ion batteries, *J. Power Sources*, 2021, **496**, 229759.

24 Y. Li, *et al.*, Enhancing high rate performance and cyclability of LiFePO4 cathode materials for lithium ion batteries by boron doping, *J. Alloys Compd.*, 2021, **880**, 160560.

25 Y. Li, *et al.*, Synthesis of LiFePO4 nanocomposite with surface conductive phase by Zr doping with Li excess for fast discharging, *J. Electrochem. Soc.*, 2019, **166**(2), A410.

26 B. Zhang, *et al.*, One-pot synthesis of LiFePO4/N-doped C composite cathodes for Li-ion batteries, *Materials*, 2022, **15**(14), 4738.

27 W.-C. Chien, *et al.*, Modifying the morphology and structure of graphene oxide provides high-performance LiFePO4/C/rGO composite cathode materials, *Adv. Powder Technol.*, 2020, **31**(11), 4541–4551.

28 S. Khan, *et al.*, Surfactant-mediated and morphology-controlled nanostructured LiFePO4/carbon composite as a promising cathode material for Li-ion batteries, *ChemistryOpen*, 2020, **9**(1), 23–31.

29 N. Algethami, *et al.*, Preparation of RuO2/CNTs by Atomic Layer Deposition and its application as binder free Cathode for polymer based Li-O2 battery, *Int. J. Electrochem. Sci.*, 2022, **17**, 221191.

30 Y. Liu, *et al.*, Ni-doped LiFePO4/C as high-performance cathode composites for Li-ion batteries, *Ceram. Int.*, 2020, **46**(10), 14857–14863.

31 Y. Peng, *et al.*, LiFePO 4/C twin microspheres as cathode materials with enhanced electrochemical performance, *RSC Adv.*, 2023, **13**(10), 6983–6992.

32 C. U. Mulik, *et al.*, Impact of Cu doping on the electrochemical properties of LiFePO 4 synthesized via the solution combustion method, *New J. Chem.*, 2025, **49**(23), 9609–9616.

33 X. Yan, *et al.*, Control and influence of morphology, particle size and structure of LiFePO4 on its properties, *Solid State Ionics*, 2024, **410**, 116535.

34 P. Guan, *et al.*, Recent progress of surface coating on cathode materials for high-performance lithium-ion batteries, *J. Energy Chem.*, 2020, **43**, 220–235.

35 Z. Cao, *et al.*, Biological phytic acid guided formation of monodisperse large-sized carbon@ LiFePO4/graphene composite microspheres for high-performance lithium-ion battery cathodes, *Chem. Eng. J.*, 2018, **351**, 382–390.

36 X. Huang, K. Chen and Y. Liu, Interfacial effect of nano Al2O3 modifying LiFePO4 to improve capacity retention and rate capability of lithium ion batteries, *Mater. Res. Express*, 2018, **6**(1), 015511.

37 P. Mathur, *et al.*, In situ metal organic framework (ZIF-8) and mechanofusion-assisted MWCNT coating of LiFePO4/C composite material for lithium-ion batteries, *Batteries*, 2023, **9**(3), 182.

38 Y.-W. Wang, *et al.*, Synergistic N/Mn codoping deagglomerate carbon coating of LiFePO4/C to boost electrochemical performance, *ACS Appl. Mater. Interfaces*, 2024, **16**(26), 33723–33732.

39 S.-J. Yang, *et al.*, Oxygen-induced thermal runaway mechanisms of Ah-level solid-state lithium metal pouch cells, *Etransportation*, 2023, **18**, 100279.

40 Y. L. Liao, *et al.*, Ultrafast Li-Rich Transport in Composite Solid-State Electrolytes, *Adv. Mater.*, 2025, **37**(10), 2419782.

41 S. Li, *et al.*, A dynamically stable mixed conducting interphase for all-solid-state lithium metal batteries, *Adv. Mater.*, 2024, **36**(3), 2307768.

42 Y.-L. Liao, *et al.*, Integrated interface configuration by in-situ interface chemistry enabling uniform lithium deposition in all-solid-state lithium metal batteries, *J. Energy Chem.*, 2023, **80**, 458–465.

43 S. J. Yang, *et al.*, Intrinsically Safe Lithium Metal Batteries Enabled by Thermo-Electrochemical Compatible In Situ Polymerized Solid-State Electrolytes, *Adv. Mater.*, 2024, **36**(35), 2405086.

44 X. L. Wang, *et al.*, A Robust Dual-Layered Solid Electrolyte Interphase Enabled by Cation Specific Adsorption-Induced Built-In Electrostatic Field for Long-Cycling Solid-State Lithium Metal Batteries, *Angew. Chem., Int. Ed.*, 2025, **64**(10), e202421101.

45 K. Tasaki, *et al.*, Decomposition of lipf6and stability of pf 5 in li-ion battery electrolytes: Density functional theory and molecular dynamics studies, *J. Electrochem. Soc.*, 2003, **150**(12), A1628.

46 Q.-f. Zhao, *et al.*, Surface modification of LiFePO4 by coatings for improving of lithium-ion battery properties, *Int. J. Electrochem. Sci.*, 2022, **17**(11), 221142.

47 D. Zhu, *et al.*, Investigation of the degradation of lipf6–in polar solvents through deep potential molecular dynamics, *J. Phys. Chem. Lett.*, 2024, **15**(15), 4024–4030.

48 A. Belous, I. Lisovskyi and V. Khomenko, Surface modification of cathode materials with functional coatings for enhanced lithium-ion battery durability, *J. Appl. Electrochem.*, 2025, 1–34.

49 B. Wang, *et al.*, A Hierarchical Porous C@ LiFePO 4/Carbon Nanotubes Microsphere Composite for High-Rate Lithium-Ion Batteries: Combined Experimental and Theoretical Study, *Adv. Energy Mater.*, 2016, **6**, 1600426.

50 J.-G. Han, *et al.*, An electrolyte additive capable of scavenging HF and PF5 enables fast charging of lithium-ion batteries in LiPF6-based electrolytes, *J. Power Sources*, 2020, **446**, 227366.

51 D. R. Zywotko and S. M. George, Thermal atomic layer etching of ZnO by a "Conversion-Etch" mechanism using sequential exposures of hydrogen fluoride and trimethylaluminum, *Chem. Mater.*, 2017, **29**(3), 1183–1191.

52 E. R. Østli, *et al.*, Limitations of ultrathin Al2O3 coatings on LNMO cathodes, *ACS omega*, 2021, **6**(45), 30644–30655.

53 D. Weber, *et al.*, Surface modification strategies for improving the cycling performance of Ni-rich cathode materials, *Eur. J. Inorg. Chem.*, 2020, **2020**(33), 3117–3130.

54 D. Zuo, *et al.*, Comparative study of Al2O3-coated LiCoO2 electrode derived from different Al precursors: uniformity, microstructure and electrochemical properties, *Electrochim. Acta*, 2015, **178**, 447–457.

55 S. Tajimi, *et al.*, Enhanced electrochemical performance of LiFePO4 prepared by hydrothermal reaction, *Solid state ionics*, 2004, **175**(1–4), 287–290.

56 C. A. Bezerra, *et al.*, High-purity LiFePO4 prepared by a rapid one-step microwave-assisted hydrothermal synthesis, *J. Mater. Sci.*, 2021, **56**(16), 10018–10029.

57 L. Vasquez-Elizondo, *et al.*, Urea decomposition enhancing the hydrothermal synthesis of lithium iron phosphate powders: Effect of the lithium precursor, *Adv. Powder Technol.*, 2017, **28**(6), 1593–1602.

58 D. V. Trinh, *et al.*, Hydrothermally synthesized nanostructured LiMnxFe$_{1-x}$PO4 (x= 0–0.3) cathode materials with enhanced properties for lithium-ion batteries, *Sci. Rep.*, 2021, **11**(1), 12280.

59 Y. Zhang, *Study on Electronic Structure and Rate Performance of Olivine Phosphate Cathode Materials*, Queensland University of Technology, 2020.

60 B. Jin and H.-B. Gu, Preparation and characterization of LiFePO4 cathode materials by hydrothermal method, *Solid State Ionics*, 2008, **178**(37–38), 1907–1914.

61 Z. Li, *et al.*, Advanced mechanisms and applications of microwave-assisted synthesis of carbon-based materials: a brief review, *Nanoscale Adv.*, 2025, 419–432.

62 S. Liu, *et al.*, One-step microwave synthesis of micro/nanoscale LiFePO4/graphene cathode with high performance for lithium-ion batteries, *Front. Chem.*, 2020, **8**, 104.

63 M.-S. Song, *et al.*, Simple and fast synthesis of LiFePO4-C composite for lithium rechargeable batteries by ball-milling and microwave heating, *J. Power Sources*, 2007, **166**(1), 260–265.

64 K. Park, *et al.*, Synthesis of LiFePO4 by co-precipitation and microwave heating, *Electrochem. Commun.*, 2003, **5**(10), 839–842.

65 W. Li, *et al.*, Preparation and characterization of LiFePO 4 from NH 4 FePO4·H2O under different microwave heating conditions, *J. Solid State Electrochem.*, 2007, **11**, 799–803.

66 Y.-J. Lv, *et al.*, Synthesis of bowl-like mesoporous LiFePO4/C composites as cathode materials for lithium ion batteries, *Electrochim. Acta*, 2014, **119**, 155–163.

67 S. Weng, *et al.*, A carbothermal reduction method for enhancing the electrochemical performance of LiFePO4/C composite cathode materials, *Ionics*, 2013, **19**(2), 235–243.

68 S.-B. Lee, *et al.*, Synthesis of LiFePO4 material with improved cycling performance under harsh conditions, *Electrochem. Commun.*, 2008, **10**(9), 1219–1221.

69 H. Kuo, *et al.*, Effect of LiI amount to enhance the electrochemical performance of carbon-coated LiFePO4, *Electrochem. Solid-State Lett.*, 2009, **12**(6), A111.

70 H. Raj and A. Sil, Effect of carbon coating on electrochemical performance of LiFePO 4 cathode material for Li-ion battery, *Ionics*, 2018, **24**, 2543–2553.

71 L. Chen, *et al.*, Biosynthesis of LiFePO4/C cathode materials by a sol-gel route for use in lithium ion batteries, *Int. J. Electrochem. Sci.*, 2019, **14**(3), 2846–2856.

72 L. Chen, *et al.*, Effects of citric acid on the preparation of a LiFePO4@ C cathode material assisted by biomineralization, *Int. J. Electrochem. Sci.*, 2019, **14**(8), 8048–8057.

73 D. Meng, *et al.*, Lithium iron phosphate with high-rate capability synthesized through hydrothermal reaction in low Li concentration solution, *J. Alloys Compd.*, 2023, **967**, 171570.

74 D. Vernardou, Recent report on the hydrothermal growth of LiFePO4 as a cathode material, *Coatings*, 2022, **12**(10), 1543.

75 P. Benedek, *et al.*, Low temperature hydrothermal synthesis of battery grade lithium iron phosphate, *RSC Adv.*, 2017, **7**, 17763–17767.

76 M. Lin, *et al.*, Hydrothermal synthesis of corn cob-like LiFePO4/C as high performance cathode material for lithium ion batteries, *Adv. Sci. Technol.*, 2014, **93**, 152–157.

77 P. N. Shirbhate, A. V. Deshmukh and V. B. Shivkumar, Rapid microwave tissue processing and staining method using a kitchen microwave oven in histopathology laboratory: A comparative study with routine histoprocessing method, *Med. J. Babylon.*, 2022, **19**(3), 383–390.

78 Z. Jiang, *et al.*, A sustainable strategy for spent Li-ion battery regeneration: microwave-hydrothermal relithiation complemented with anode-revived graphene to construct a LiFePO 4/MWrGO cathode material, *Sustainable Energy Fuels*, 2022, **6**(9), 2207–2222.

79 D. Grekov, P. Pré and B. J. Alappat, Microwave mode of heating in the preparation of porous carbon materials for adsorption and energy storage applications–an overview, *Renewable Sustainable Energy Rev.*, 2020, **124**, 109743.

80 G. Cheruvally, *Lithium Iron Phosphate: A Promising Cathode-Active Material for Lithium Secondary Batteries*, 2008.

81 Z. Chen, Q. Zhang and Q. Liang, Carbon-coatings improve performance of Li-ion battery, *Nanomaterials*, 2022, **12**(11), 1936.

82 H. Li and H. Zhou, Enhancing the performances of Li-ion batteries by carbon-coating: present and future, *Chem. Commun.*, 2012, **48**(9), 1201–1217.

83 J. Choi, *et al.*, Advancing structural batteries: cost-efficient high-performance carbon fiber-coated LiFePO 4 cathodes, *RSC Adv.*, 2023, **13**(44), 30633–30642.

84 M. A. Syed, M. Salehabadi and M. Obrovac, High energy density large particle LiFePO4, *Chem. Mater.*, 2024, **36**(2), 803–814.

85 S. Anandan, R. Vijay, and T. N. Rao, *Method of Producing In-Situ Carbon Coated Lithium Iron Phosphate Cathode Material for Lithium-Ion Batteries and the Product Thereof, Google Patents*, 2024.

86 L. Wang, *et al.*, Preparation of LiFePO4 composite based on dual carbon sources of phytic acid and glucose and its

performance for lithium extraction from salt lake, *Sep. Purif. Technol.*, 2023, **306**, 122605.

87 H. Rostami, *et al.*, Life cycle of LiFePO4 batteries: production, recycling, and market trends, *ChemPhysChem*, 2024, **25**(24), e202400459.

88 Z. Chen and J. Dahn, Reducing carbon in LiFePO4/C composite electrodes to maximize specific energy, volumetric energy, and tap density, *J. Electrochem. Soc.*, 2002, **149**(9), A1184.

89 S. Bewlay, *et al.*, Conductivity improvements to spray-produced LiFePO4 by addition of a carbon source, *Mater. Lett.*, 2004, **58**(11), 1788–1791.

90 Y.-D. Cho, G. T.-K. Fey and H.-M. Kao, The effect of carbon coating thickness on the capacity of LiFePO4/C composite cathodes, *J. Power Sources*, 2009, **189**(1), 256–262.

91 A. V. Murugan, T. Muraliganth and A. Manthiram, One-pot microwave-hydrothermal synthesis and characterization of carbon-coated LiMPO4 (M= Mn, Fe, and Co) cathodes, *J. Electrochem. Soc.*, 2008, **156**(2), A79.

92 Y.-K. Kwon and P. Kim, Unusually high thermal conductivity in carbon nanotubes, *High Thermal Conductivity Materials*, 2006, pp. 227–265.

93 D. Yang, *et al.*, Thermal and electrical transport in multi-walled carbon nanotubes, *Phys. Lett. A*, 2004, **329**(3), 207–213.

94 Z.-Y. Chen, *et al.*, Electrochemical performance of carbon nanotube-modified LiFePO4 cathodes for Li-ion batteries, *Trans. Nonferrous Met. Soc. China*, 2010, **20**(4), 614–618.

95 J. Xu, G. Chen and X. Li, Electrochemical performance of LiFePO4 cathode material coated with multi-wall carbon nanotubes, *Mater. Chem. Phys.*, 2009, **118**(1), 9–11.

96 H. An and K. Park, LFP via Nanoscale Surface Reforming with a Tiny Minimal Amount of Conductivity-Enhancing Material, *Langmuir*, 2025, 1821–1829.

97 G. Qin, Q. Ma and C. Wang, A new route for synthesizing C/LiFePO4/multi-walled carbon nanotube secondary particles for lithium ion batteries, *Solid State Ionics*, 2014, **257**, 60–66.

98 X. Jiang, *et al.*, Effect of heteroatom doping on electrochemical properties of olivine LiFePO4 cathodes for high-performance lithium-ion batteries, *Materials*, 2024, **17**(6), 1299.

99 N. Shaji, *et al.*, Heteroatoms-doped carbon effect on LiFePO4 cathode for Li-ion batteries, *J. Energy Storage.*, 2023, **72**, 108710.

100 Q. Xiong, *et al.*, Nitrogen-doped carbon shell on metal oxides core arrays as enhanced anode for lithium ion batteries, *J. Alloys Compd.*, 2016, **688**, 729–735.

101 K. Mi, *et al.*, Sole chemical confinement of polysulfides on nonporous nitrogen/oxygen dual-doped carbon at the kilogram scale for lithium–sulfur batteries, *Adv. Funct. Mater.*, 2017, **27**(1), 1604265.

102 Q. Chen, *et al.*, Nitrogen-doped carbon layer of LiFePO4 improves the electrochemical performance for lithium ion batteries, *Ionics*, 2023, **29**(11), 4537–4545.

103 Q. Xiong, *et al.*, Controllable synthesis of NC@ LiFePO4 nanospheres as advanced cathode of lithium ion batteries, *J. Alloys Compd.*, 2018, **743**, 377–382.

104 S. Wang and F. Wang, Effect of Mn, N co-doped LiFePO4 on electrochemical and mechanical properties: A DFT study, *J. Mol. Graphics Modell.*, 2023, **125**, 108604.

105 Z. Cui, *et al.*, Synergy of structural engineering and dual-heteroatoms co-doping engineering boosting porous carbon toward efficient capacitive deionization, *Desalination*, 2024, **572**, 117122.

106 Y. Yang, K. Li and H. Li, Doping effects on the crystal structure and electrochemical performance of LiFePO4/C, *Int. J. Appl. Ceram. Technol.*, 2015, **12**(1), 163–168.

107 J. P. Mwizerwa, *et al.*, Three-dimensional printed lithium iron phosphate coated with magnesium oxide cathode with improved areal capacity and ultralong cycling stability for high performance lithium-ion batteries, *J. Colloid Interface Sci.*, 2022, **623**, 168–181.

108 R. Saroha, *et al.*, Development of surface functionalized ZnO-doped LiFePO4/C composites as alternative cathode material for lithium ion batteries, *Appl. Surf. Sci.*, 2017, **394**, 25–36.

109 P. Salimi, *et al.*, Improving lithium-ion battery performance: nano Al2O3 coatings on high-mass loading LiFePO4 cathodes via atomic layer deposition, *Batteries*, 2024, **10**(9), 304.

110 Y. Xu and J. Mao, Enhanced electrochemical performance of LiFePO4 cathode with carbon-TiO2 hybrid coating, *J. Mater. Sci.*, 2016, **51**(22), 10026–10034.

111 J. Shi, *et al.*, ZrO2 and nitrogen-doped carbon Co-coated LiFePO4 cathode with improved cycling stability and rate performance for lithium batteries, *J. Wuhan Univ. Technol., Mater. Sci. Ed.*, 2022, **37**(6), 1073–1079.

112 Z. Sun, *et al.*, High-Performance Silicon Anodes Enabled by Multifunctional Ultrafine Silica Nanoparticle-Embedded Carbon Coatings for Lithium-Ion Batteries, *Adv. Energy Mater.*, 2025, 2500189.

113 L. Tong, *et al.*, Improvement of electrochemical properties of lithium iron phosphate cathode by rare earth oxides modification, *J. Alloys Compd.*, 2023, **947**, 169581.

114 G. Zhang, *et al.*, Lithium iron phosphate and layered transition metal oxide cathode for power batteries: attenuation mechanisms and modification strategies, *Materials*, 2023, **16**(17), 5769.

115 P. Salimi, G. Gottardi, W. G. Morais, R. Bartali, N. Laidani and E. G. Macchi, Improving lithium-ion battery performance: nano Al2O3 coatings on high-mass loading LiFePO4 cathodes via atomic layer deposition, *Batteries*, 2024, **10**(9), 304.

116 T. Feng, *et al.*, Low-cost Al2O3 coating layer as a preformed SEI on natural graphite powder to improve coulombic efficiency and high-rate cycling stability of lithium-ion batteries, *ACS Appl. Mater. Interfaces*, 2016, **8**(10), 6512–6519.

117 L. Hou and G. Tao, A first-principles study of bulk and surface Sn-doped LiFePO4: The role of intermediate valence component in the multivalent doping, *Phys. Status Solidi B*, 2017, **254**(10), 1700041.

118 M. R. Laskar, *et al.*, Atomic layer deposition of Al2O3–Ga2O3 alloy coatings for Li [Ni0. 5Mn0. 3Co0. 2] O2

cathode to improve rate performance in Li-Ion battery, *ACS Appl. Mater. Interfaces*, 2016, **8**(16), 10572–10580.

119 Y.-S. Lee, *et al.*, Improvement of the cycling performance and thermal stability of lithium-ion cells by double-layer coating of cathode materials with Al2O3 nanoparticles and conductive polymer, *ACS Appl. Mater. Interfaces*, 2015, **7**(25), 13944–13951.

120 S. Hao and C. Wolverton, Lithium transport in amorphous Al2O3 and AlF3 for discovery of battery coatings, *J. Phys. Chem. C.*, 2013, **117**(16), 8009–8013.

121 L. Wang, *et al.*, Enhanced electrochemical properties of LiFePO4/C cathode material by metal oxide coating, *Adv. Mater. Res.*, 2012, **347**, 3443–3447.

122 X. L. Wu, *et al.*, Carbon-nanotube-decorated nano-LiFePO4@ C cathode material with superior high-rate and low-temperature performances for lithium-ion batteries, *Adv. Energy Mater.*, 2013, **3**(9), 1155–1160.